

Buckling of Thin Cylindrical Shells with a Creased Surface

Alejandro Gómez Gómez

Supervisor: Dr Martin Walker

Department of Engineering Science &
University College, University of Oxford

Introduction

This project investigates the buckling behaviour of thin cylindrical shells when compressed axially. The shells' imperfection-sensitivity is studied and the cross section of the cylindrical shells is altered to try and control this sensitivity to imperfections, seeking to increase the shells' critical buckling load to get closer to the values predicted by the classical theory. The project consists of two parts: the experimental testing and the numerical analysis. For the experimental testing part, a corrugating machine is designed and built to corrugate the shells by adding creases to them. The shells are then tested during axial compression using an INSTRON 5582 machine. The numerical analysis is performed using the Finite Element Analysis software ABAQUS, to simulate the axial compression of the shells.

Experimental Testing

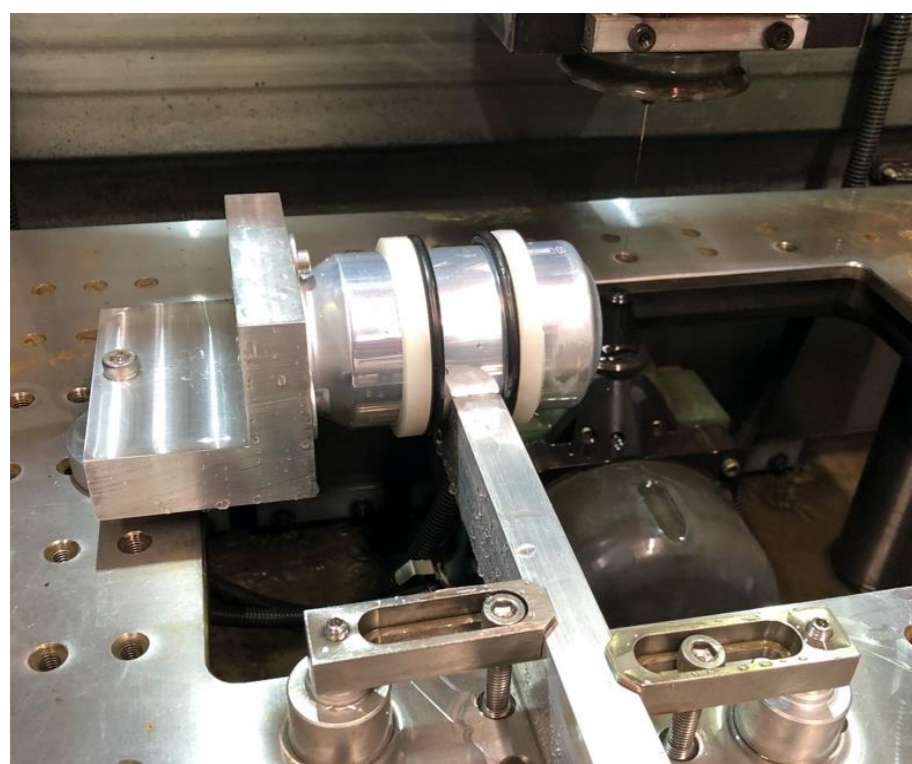


Figure 1 – Beverage can setup in EDM machine

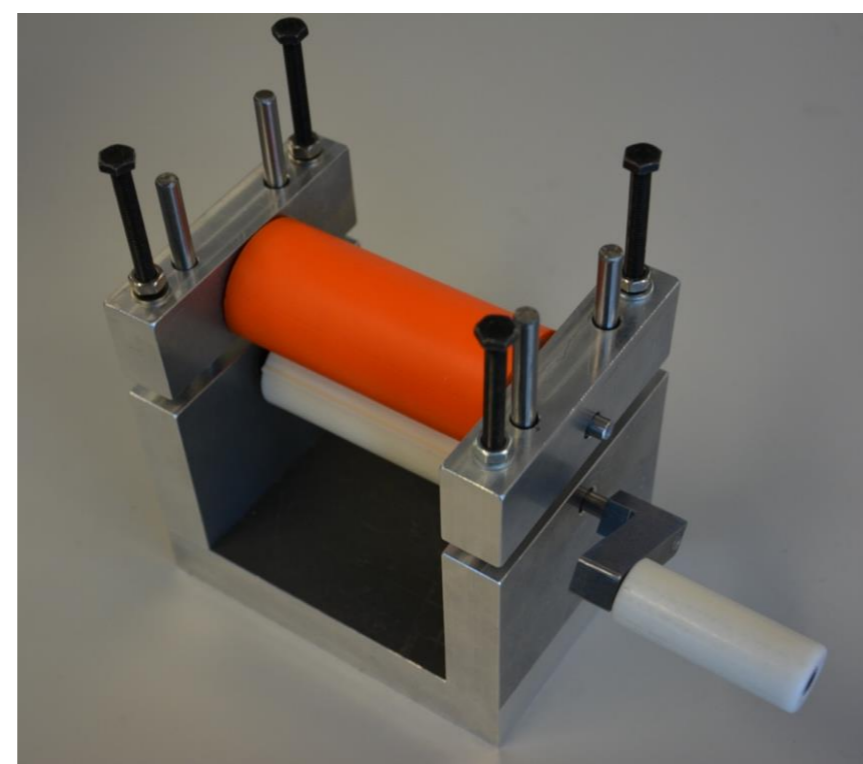


Figure 2 – Corrugating machine

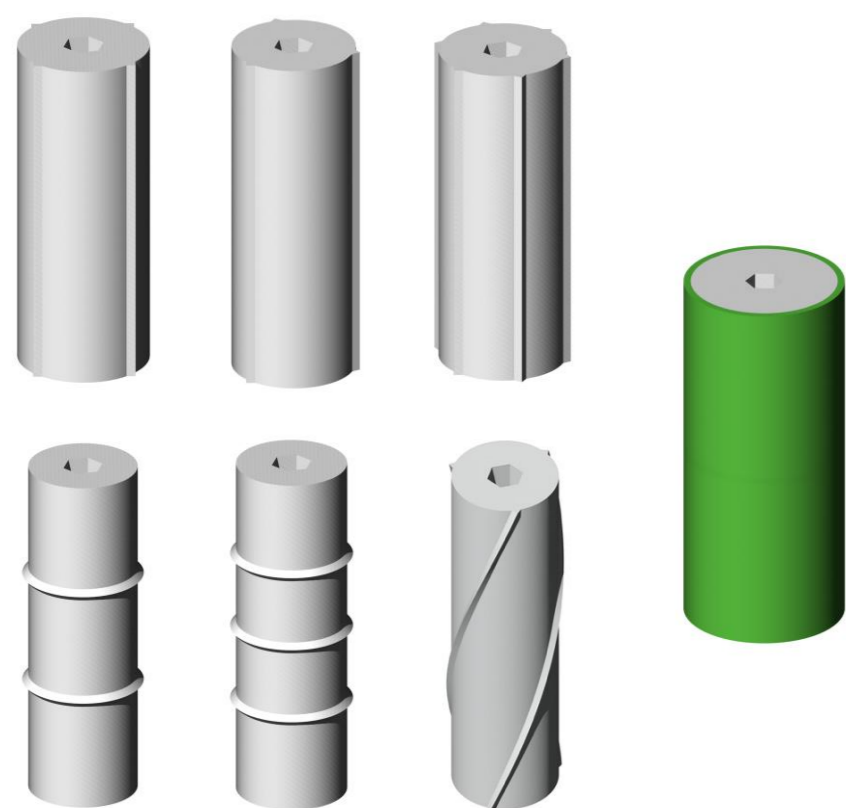


Figure 3 – Different crease rollers



Figure 4 – Different shell crease patterns

The cylindrical shells used for this experiment were made from regular unused beverage cans, by removing the top and bottom ends. The AgieCharmilles Cut P 350 machine from the University of Oxford Engineering Department was used to cut the cans, as shown in Figure 1. It uses Electrical Discharge Machining (EDM), whereby the material of the can is removed by a series of rapidly recurring current discharges between two wires that act as electrodes. The cans were cut to cylindrical shells with dimensions: $t = 0.12 \text{ mm}$ $r = 32.5 \text{ mm}$ $l = 80.0 \text{ mm}$

In order to impose creases on the samples, a corrugating machine was designed and built, as shown in Figure 2. The two rollers are connected to the stands by an axle with a hexagonal cross-section, one of which has a crank handle at the end to ensure an easy rotation. One roller is corrugated and the other is a rubber roller. To corrugate each sample, the sample is placed around one of the rollers and pressed against the other. To get an inner-crease pattern, the sample is placed around the rubber roller, so that the corrugating roller presses the triangular extrusions against it from the outside, and to get an outer-crease pattern, it's vice versa. Then, the screws are screwed downwards, until the sample is firmly pressed against both rollers, and a 720 degrees rotation is applied to create the creases, as the circumference of the rollers is half of that of the cylindrical shells. Figure 3 shows the different types of rollers used to create different types of corrugated shells, shown in Figure 4. Tests were conducted on the six, eight and twelve-crease cylindrical shells, both for the inner and outer cases. Three samples were tested for each different crease pattern. The buckling tests were performed using an INSTRON 5582 machine, where the samples were compressed between two circular plates, and in order to enforce pinned boundary conditions, P100 sandpaper was cut into circles and stuck onto each plate. The theoretical classical buckling load for the samples according to its material properties and dimensions is $N_{cl} = 3874 \text{ N}$.

The FEA software used to simulate the axial compression of the different types of samples is ABAQUS (2018). To model this type of problem a large-displacement nonlinear static stress analysis was used. The exact dimensions of the samples, including their crease patterns, were found using a 3D Scanner. Each FEA analysis was performed for a perfect and imperfect type shell. The imperfections were added by superposing the critical buckling eigenmode shapes onto the shell.

In the following sections the results for several types of crease patterns are presented, both for the experimental testing and the FEA analysis.

Conclusion

There are several key similarities observed between the results obtained from experimental testing and the FEA models. The inner-crease shells obtained a higher peak buckling load than their outer-crease counterparts when tested in real life. The same can be said for the FEA shell models. This confirms that inner creases are more effective in increasing the load-carrying capacity of a shell, and further investigation on the subject should be focused on inner creases. When comparing the outer-crease experiments, the higher the number of creases, the higher the peak buckling load. However, if the inner-crease experiments are compared, the lower the number of creases, the higher the peak buckling load. The FEA results agree for the outer-crease shells, but in the case of the inner-crease shells, the higher the number of creases, the larger the peak buckling load. So the FEA results conclude that higher crease number shells will have a larger peak buckling load and knockdown factor. The post-buckling loads for the FEA results are roughly about twice the size than the post-buckling loads for the actual samples. However, both agree in that the post-buckling load remains fairly similar in value regardless of the crease pattern.

When observing the buckling modes for the FEA models, it can be seen that they resemble the real samples' buckling modes. When observing Figures 7 and 11, it can be seen that the twelve-inner-crease shells buckle by forming large diamond-shaped dimples that are as long as the height of the shell, where the FEA results agree with the experimental results. The FEA results also agree with the experimental results in that the outer creases in the cylinders disrupt the diamond-shaped dimple pattern, as seen in Figures 6 and 10. The outer-crease shells obtained a low peak buckling load, which is unexpected as it was thought that the disruption of the dimples would increase the load-carrying capacity.

The expected outcome was to increase the load-carrying capacity of the shells by adding creases, which proved to be successful. All the creased shells had a higher buckling load than the non-corrugated shell. Furthermore, it was concluded that inner creases were more effective for this purpose, regardless of the crease number. However, the FEA results had some fundamental incongruences with the experimental results, mainly being that they offered an unrealistically large value for the peak buckling loads and post-buckling loads.

Structural engineers have an obligation to contribute to reducing embedded carbon in the built environment. By reducing the thickness of cold-formed, thin-walled structural elements, material use can be reduced. In order to accomplish this greater control over buckling imperfection sensitivity is critical. Texturing has the potential to address this need. Despite this project focusing on cylindrical shells, the result could also apply to other thin-walled shapes. Additionally, this project could open the possibility of controlling the buckling process upon further study, with potential applications in energy dissipating systems, and deployable structures.

Experimental Results

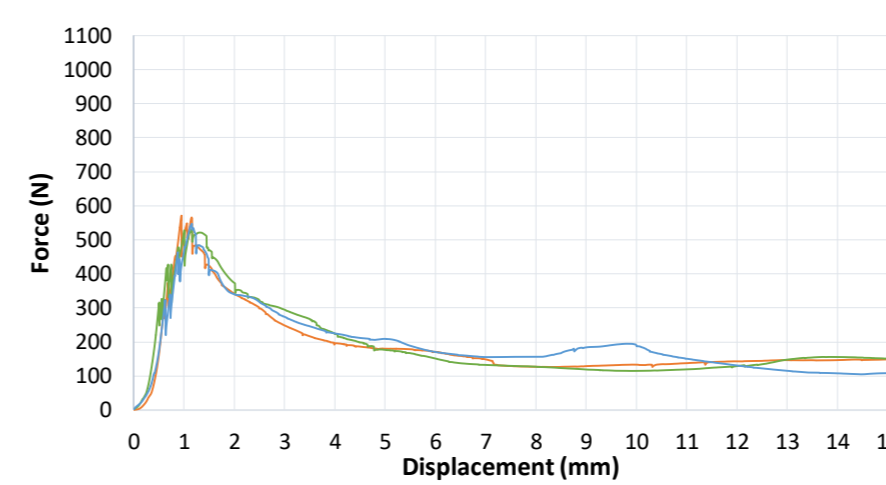


Figure 5 – Axial compression for non-corrugated cylinders

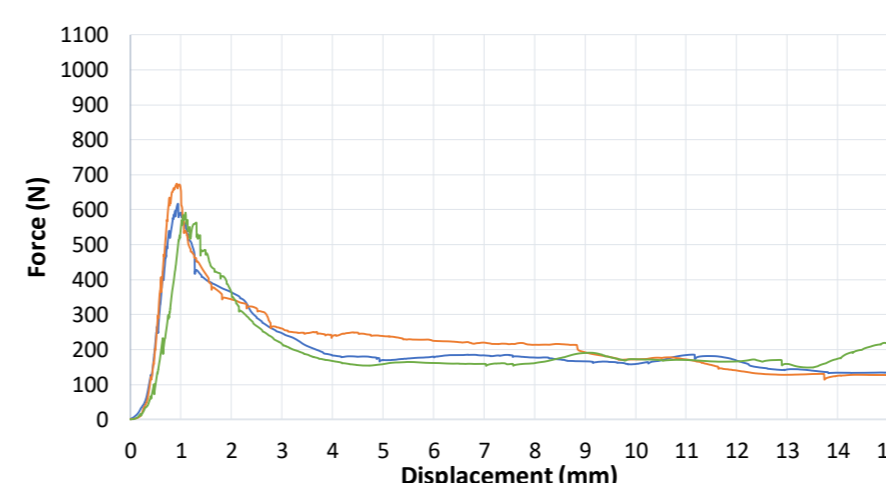


Figure 6 – Axial compression for eight-outer-crease cylinders

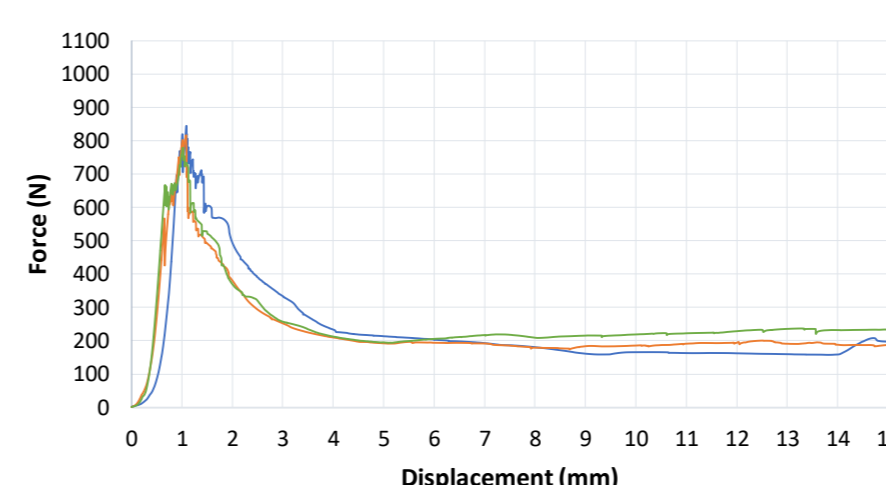


Figure 7 – Axial compression for twelve-inner-crease cylinders

Finite Element Analysis

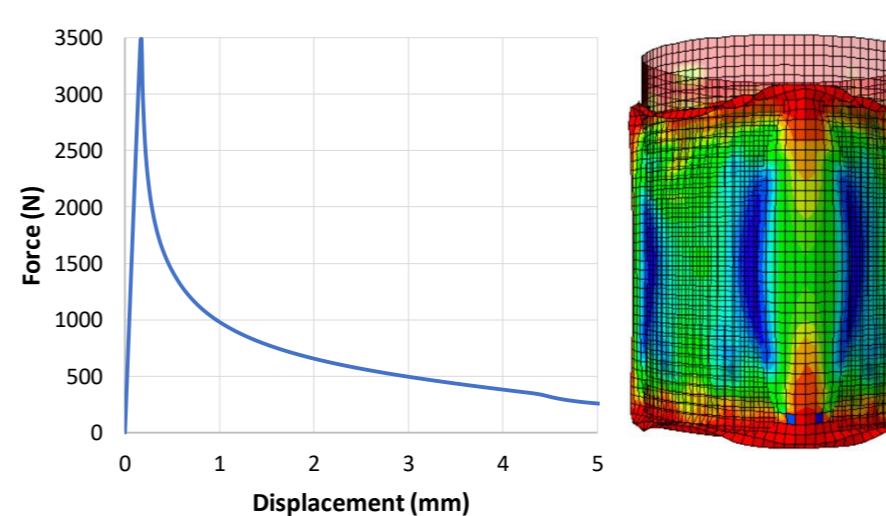


Figure 8 – FEA axial compression of a perfect non-corrugated shell

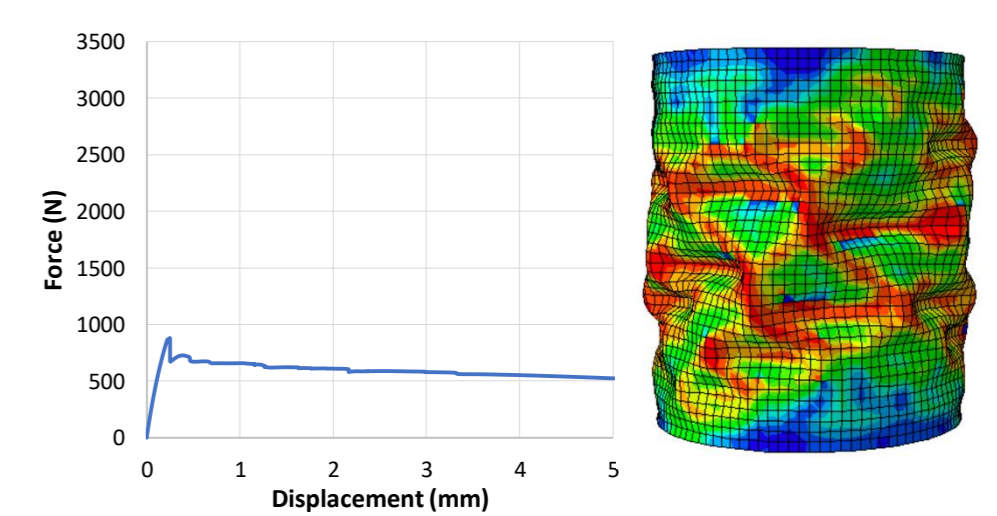


Figure 9 – FEA axial compression of a non-corrugated shell with imperfections

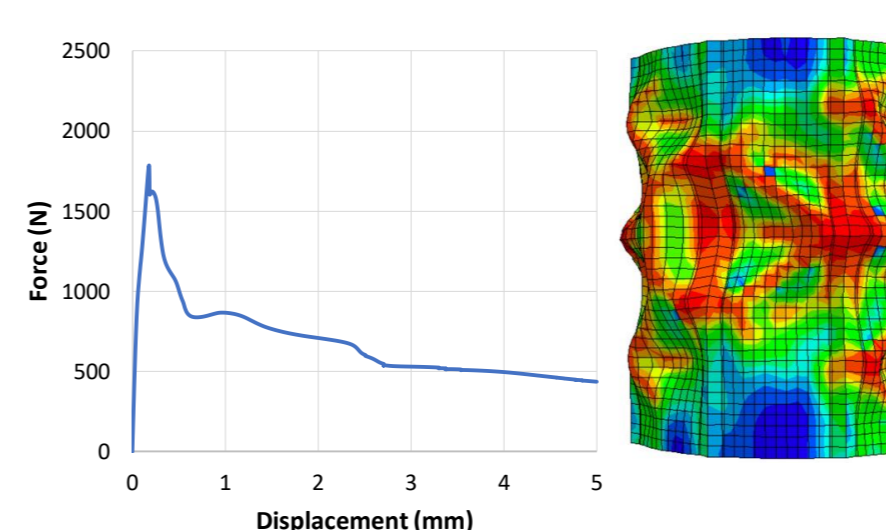


Figure 10 – FEA axial compression of an eight-outer-crease shell with imperfections

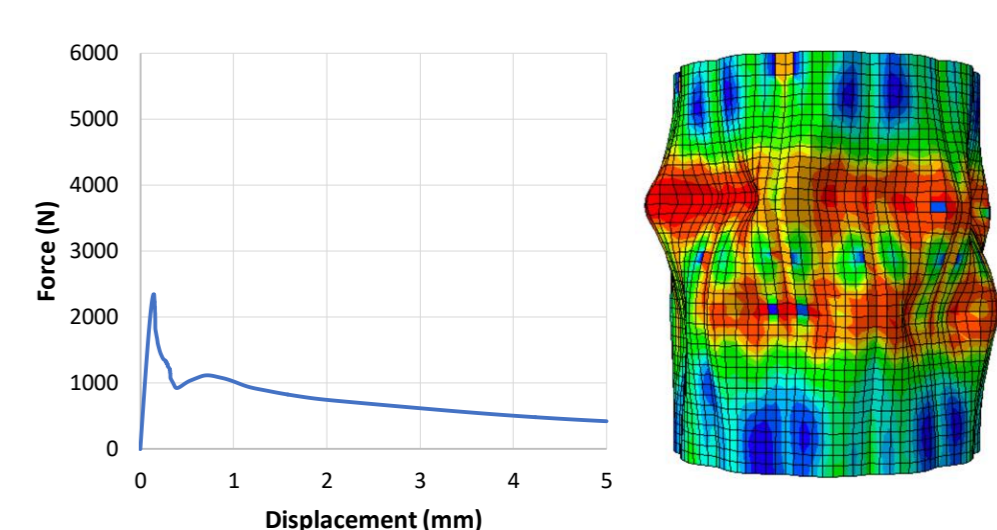


Figure 11 – FEA axial compression of a twelve-inner-crease shell with imperfections

Shell type	Experimental			FEA		
	Peak buckling load N_b (N)	γ	Post-buckling load (N)	Peak buckling load N_b (N)	γ	Post-buckling load (N)
Non-corrugated	550	0.142	143	880	0.227	524
Eight-outer-crease	628	0.162	167	1786	0.461	436
Eight-inner-crease	945	0.244	164	2277	0.588	394
Twelve-outer-crease	703	0.181	165	2055	0.530	557
Twelve-inner-crease	813	0.210	197	2347	0.606	423
Six-outer-crease	538	0.139	159	1476	0.381	488
Six-inner-crease	1016	0.261	189	1748	0.451	406

Table 1 – Results from the experimental testing and ABAQUS imperfect shells analyses